Friction and wear behavior of femtosecond laser nanotextured metallic surfaces lubricated with graphene

Ricardo Jorge Clemente Martins

Rjcm2015@gmail.com

Instituto Superior Técnico, Universidade de Lisboa, Portugal

October 2020

This work is focused on studying the friction and wear behavior of LIPSS (Laser-Induced Periodic Surface Structures) textured steel surfaces coated with solid lubricants graphene oxide (GO) and graphene (Gr).
The femtosecond laser that used for nanotexturing the steel surfaces has a wavelength of 1024 nm and gaussian energy distribution. Samples were textured with LIPSS, and the orientation attained was perpendicular to the polarization direction of the laser beam. The LIPSS have an average period of 1,4 µm between grooves, a Mean Profile Depth of 0,202 µm (MPD), and an average Ra=0,220 µm. Tribological tests were carried out on textured and polished samples, using a nanotribometer, in a sphere-on-plane configuration, with alternating linear sliding movement, parallel and perpendicular to the LIPSS orientation. The as-textured surfaces present lower friction coefficients, ranging from 0.9 to 0.7. Coating with GO or Gr reduces considerably the friction coefficient, the highest reduction being attained for Gr-coated surfaces between [0.3; 0.4]. The friction coefficient is lower when sliding in a direction parallel to the LIPSS orientation than in the perpendicular direction.

Keywords: LIPSS textures; Graphene Oxide (GO); Graphene (Gr); Tribology.

1. Introduction

Although tribological concepts are much older than its industry, it has always been connected to industrial problems since their birth. Tribology establishes relationships between phenomena such as friction, wear, and lubrication for different types of mechanical contacts. These types of studies are necessary to ensure the safety and performance of any equipment. As stated in Popov (2018), concepts like tribology are described in numerous papers. Nevertheless, it is still unknown or has relatively low visibility among both the engineering field and the general public despite its essential role in the industrial world as well as in everyday life.[1] With the necessity for better-quality or specific lubricants: lubricants with longer lifetimes, less friction (less wear), more environmentally friendly or that could be applied in distinct fields/industries that command a considerable amount of capital opening the door for new studies or new lubricants both, solid and liquid. The development and discovery of new materials like graphene that fills all the requirements mentioned above support the creation of this work. LIPSS is a phenomenon where there is a change in the surface topography by means of laser radiation. This technology has been increasingly used in providing color for technical surfaces[2], the control of surface wetting,[3] the tailoring of surface colonization by bacterial biofilms, [4] and the improvement of the tribological performance of nanostructured metal surfaces[5]. LIPSS can take different forms and shapes, which means it requires a profound analysis of each application. One of the most vital and used technologies in manufacturing industries is laser technology. A combination between high-speed manufacture, excellent control of the shape and size of the patterns, ability to reduced material waste, and the ability to create complex parts or segments, makes this type of equipment, without a doubt, a wonder of the twenty-first century. We chose femtosecond laser for this work because of his unique capability to use an ultrashort pulse width, an electromagnetic pulse whose time duration is of the order of 10^{-15} seconds, and ultrahigh peak power that can safely process almost all material. Since FS laser is ideal to be used in surface texturing for tribological applications because it provides us with exceptional control, we expect to minimize the melt ejection and heat-affected zones (HAZ). After the discovery of 2D materials, especially graphene, a carbon-based material, a new light was shined in the lubricant industry. With this in mind, we decided to study the influence that graphene-based solid lubricant has on LIPSS tribological properties.[6]

1.1. Motivation

My motivation for this work is that there are many open questions remaining, concerning fields like tribology, with regarding new emergent materials. So, creating knowledge, developing, testing, and validating new techniques/methods are the most critical aspects for a materials engineering student like me. The second is the necessity of reducing energy loss in several industries. Kenneth Holmberg and Ali Erdemir [7][8] stated that in total, ~23% (119 EJ) of the world's total energy consumption originates from tribological contacts. Where 20% is for overcoming friction, 3% is to remanufacture worn parts and spare equipment due to wear and wear-related failures. Also, establish that 30% of the energy in transport is to overcome friction while in the industry is about 15 – 20%. In residential and other areas, the power to overcome friction is less than 10%. With this in mind, understanding what happens at macro, micro, and nanoscale is essential and has an enormous impact on machinery reliability and performance. Thus, creating a great market and a strong request for machines that use less energy with the same output, in addition to having a better service life for the same components. Achieving such results could only be done by the development of new materials or lubricants. Since we are using lubricants in our work, it is necessary to have some information about the global lubricants market. Fast industrial advances for new materials like aluminum, metal alloys, and composites, creates high demand, with the objective to minimize inertia, weight, friction, resistance to wear and heat. Using specialized/engineered lubricants, like a graphene-based lubricant, to solve the problems of rust, wear, friction associated with materials, and to apply in specific environments and industries.[9]

1.2 Objective

The objective of this work is to study and improve the tribological behavior of tool steel surfaces textured by laser, with graphene-based lubricant. Also, understanding if LIPSS can act as a reservoir. The study focuses on tribological tests at the nanoscale on texturized tool steel surfaces. The tests done on tool steel samples with three surface finishes: (i) polished, (ii) laser textured surface, and (iii) polished and textured coated surfaces with graphene oxide (GO) or graphene (Gr). The tribological tests use a sphere-on-plane configuration, with an alternating linear sliding motion. In the samples textured by the laser, the tests were carried out both parallel and perpendicular directions to the LIPSS. The tests allow us to measure the friction coefficient under different conditions, and the surfaces were analyzed by scanning electron microscopy to identify the material removal mechanisms.

2. State of the Art

This section gives an insight of the LIPSS, materials, and techniques proposed for textured surfaces and coating deposition methods.

2.1. LIPSS

LIPSS is the change in surface topography using laser radiation and occurs when a surface treatment creates periodic ripples/grooves in a very controllable way, figure 7.[6][5] They can be divided into (LSFL) - Low spatial frequency with periods near the wavelength of the radiation and (HSFL) High spatial frequency with periods much lower than the radiation wavelength.[6] For strong absorbing materials such as metals or semiconductors in most cases, they have LSFL with a period close to or somewhat smaller than the wavelength (λ) and an orientation perpendicular to the laser beam polarization.[9][10] In dielectrics, fs-LSFL are observed either perpendicular or (for large bandgap materials) parallel to the beam polarization. Often, they show ripple periods either close to (λ) or close to $\frac{\lambda}{n}$, where n is the refractive index of the dielectric material[10].

High-spatial-frequency LIPSS (HSFL) with spatial periods significantly smaller than half of the irradiation wavelength have been observed predominantly for transparent materials and with orientations often perpendicular and sometimes parallel to the beam polarization. LSFL generation is well established and accepted by the scientific community. However, a study done by Stefan, Rung[11] links the formation of LSFL on steel surfaces with a surface finish. In a regime of higher surface roughness, he generated LSFL with orientation along with the linear polishing profile. The origin of the HSFL is controversial and discussed. To this day, there is no consensus on the respective mechanisms and formation. Changing the laser processing parameters allows us to attain LIPSS, nano-waves, nano-cones, peaks, holes, columns. Frequency and type of LIPSS (HSFL or LSFL) depend on the processing parameters used, such as wavelength and incident angle of the laser beam, number of pulses and radiation fluence, laser beam polarization, environmental conditions, and material properties.[5]

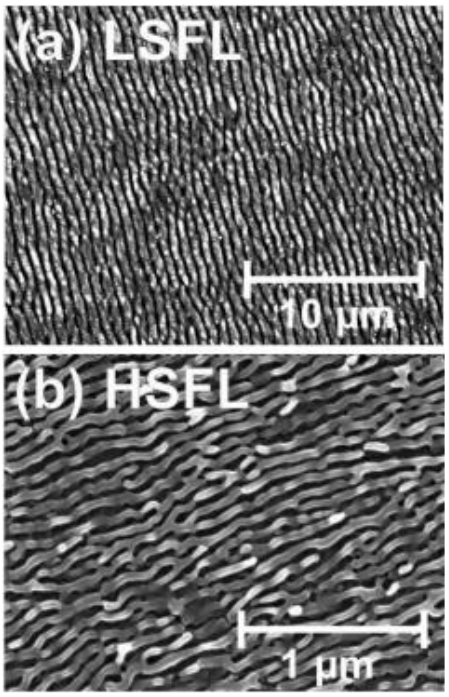

Figure 1 - SEM images of FS laser for (a) high and (b) low spatial frequency LIPSS. Image reproduced from [26].

2.2. Wettability

Wettability is one of the properties that can be enhanced by LIPSS. These structures can control surface hydrophobicity and can be explained by the increased roughness of the laser-treated surfaces and by the entrapment underneath the liquid, increasing the contact angle. Thus, the development of materials with optimized wettability may be relevant to applications in the biomedical field.[37] Generally, there are two opposite wetting behaviors. The first behavior defined by complete drying, in which a liquid droplet brought into contact with a solid surface remains spherical without developing any significant contact with its superhydrophobic surface that exhibits a water contact angle bigger than at least 150°. The second is defined by complete wetting, in which a droplet brought into contact with a solid surface spontaneously spreads and forms a film super-hydrophilic that shows a water contact angle equals or near to 0°. Intermediary behaviors can also occur, in which the droplet partially wets the surface. Therefore, it is necessary to determine which surface parameters favor these different wetting behaviors. The contact angle (CA), the angle between the tangent to the liquid surface and the surface in a point of the contact line or three phasic lines, of a liquid droplet into contact with a solid surface defines the degree of wetting.

2.3. LIPSS as reservoirs

In theory, using micro or nanoscale structures can serve as reservoirs, and have proven to be beneficial by controlling the flow of lubricants, reducing friction, and improve the load-carrying capacity between sliding components. In 1965 D. B. Hamilton, Walowit, J. A. and C. M. Allen[12] published “A theory of lubrication by micro irregularities" in 1998 Geiger, M.[13] shows that ceramic surfaces, microstructure, by laser radiation, improve the tribological properties. Jörn Bonse has taken some recognition in this area by writing some of the most cited articles[6][14][15][16][17].

2.4. Role of lubricants

Lubricants can be organic or inorganic, are introduced to reduce friction between surfaces in tribological contact and have been around for a long time. This chapter will take emphasis on some guidelines on the lubricant to better understand how solid lubricant works and which (graphene or graphene-based) could function in new technological fields.[18] The [18]most important thing to do when selecting a lubricant is to understand the environmental/specific application in which the operation takes place, temperature range, environment (outer space), presence of the reactive medium, or chemical compatibility of lubricant with the material, viscosity, etc.

2.5. Graphene and graphene-based lubricant

Attributed to the availability for chemical modification, in recent years there has been a rise in research for 2D materials like graphene, an sp2-bonded two-dimensional monolayer of carbon organized in a hexagonal lattice.[19] Graphene and her sp^2-hybridization attracted attention because of their unique and fascinating properties. For a one-atom-thick material (*3.5 Å based on the interplanar spacing of crystalline graphite), it exhibits enormous high intrinsic strength of up to 130 GPa, Young's modulus of up to 1 TPa, as well as ultra-low friction.[19] [20] In this sub-section, the friction and wear reduction of coatings facilitated by monolayer, few-layers, multi-layers, and reduced graphene oxide (rGO) is discussed, emphasizing the intrinsic advantages of graphene and the ability to be used as lubricant coating.

3. Experimental procedure

3.1. Materials

3.1.1. Tool steel

The steel used in this experimental work is DIN 90MnCrV8, oil-tempered, tempered cold-working tool steel with an austenitic structure and hardness of 58-60 HRC.

The mechanical properties of this steel are listed below in Table 1.

Table 1 - Mechanical properties of the tool steel metal.[5]

	Young modulus, E [GPa]	Poisson coefficient, v	Yield stress, σy [MPa]	Hardness
DIN 90MnCrV8	~200	~0,3	1750	58-60 HRc ~653-697 HV

3.1.2. Graphene oxide in water dispersion

Graphene oxide in water dispersion produced by Graphenea with 4mg/ml and monolayer content (at 0.5mg/ml) >95%

Table 2 - Chemical composition of graphene oxide.

%	C	H	N	S	O
	49-56	0-1	0-1	0-2	41-50

3.1.3. Graphene

Powdered graphene was manufactured by researchers from IPFN - Instituto de Plasmas e Fusão Nuclear, project **PEGASUS** - Plasma Enables and Graphene Allowed Synthesis of Unique nanoStructures.

3.2. Methods

3.2.1. Sample preparation

DIN90MnCrV8 steel samples with dimensions of approximately 1.5 cm x 1.5 cm x 2 mm (length x width x thickness) were cut from a steel block with a mechanical saw.

The first thing done was to get a flat surface. By polishing the sample with 120-2400 sandpapers, then 6 and 3 µm diamond suspensions, and finally, colloidal silica. After polishing the samples were cleaned with water and soap, and then with acetone on an ultrasound bath, for 5 minutes and dried.

3.2.2. Surface texturing

The laser used in this experimental activity was a pulsed light Yb: KYW laser (Amplitude Systèmes S-Pulse HP). This laser belongs to the solid-state laser family and is composed of one ytterbium-doped potassium and yttrium tungstate crystal with wavelength 1024 nm and gaussian distribution. The sample is 15 mm above the focal lens of 150 mm in length. The processing parameters were chosen based on a previous work by Ana Beatriz Ferreira.[5] Sample's textured at the air environment and attained LIPSS with the perpendicular orientation to the polarization direction of the laser beam[5].

3.2.3. Deposition of GO lubricant

A dilution of graphene oxide water dispersion with ethanol 1:1 was prepared and stirred for 20-30 minutes. To deposit the graphene solution, a Double action trigger gravity airbrush (KKmoon 100-240V AeróGrafo compressor professional, Pintura artística de pulverización), was used. The deposition was done at a distance of 13-15 mm from the sample, using an air output of 10 Lpm and with a nozzle diameter of 0.3 mm. The deposition was done six times for GO and 40 times for Gr. Each layer deposition dried out at air and room temperature. Each layer, the sample rotates 90 degrees to be as homogeneous as possible.

4. Results and discussion

4.1. Coating methods

Drop Casting: Drop cast deposition consists of using a syringe to drop droplets of a liquid solution on a metal surface.

This method was not suitable for our needs because the coating was dried in air or a desiccator for 24 hours, generating a uniform film with flaws/defects, figure 2 (A). Four defects were detected in the coating: (I) the boundaries of the film show some oxidation, probably due to chemical interaction between graphene oxide solution in water and the steel; (II) after drying, uncoated areas were observed; (III) small openings/absence of lubricant; (IV)

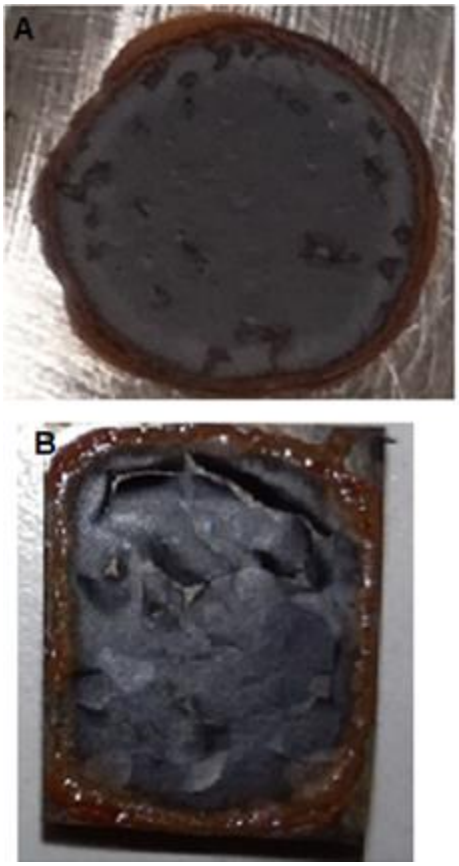

Figure 2 - GO film created by drop-casting method. (A) solid GO film and (B) Delamination of GO film.

Figure 2 (B) show numerous cracks in the GO coating, created during the drying process. During the drying process, the surface tension imposes stress, which exceeded the max stress that the thin GO film can bear. One other cause can be the poor adhesion between the GO film and surface tension produces internal stress that creates delamination.

In figure 3, it is possible to observe that the surface wettability properties favor the agglomeration between Gr sheets, making this method ineligible for our work.

Figure 3 - Graphene agglomeration attains after the drop-casting method on a polished surface.

Spray coating: This simple deposition technique uses a spray gun, like an airbrush to coat a surface. After the dried process, it is possible to see, in figure 4, some brighter and darker areas. The dark regions correspond to the GO agglomeration while the brighter zones correlate to the light reflected by the camera flash on the polished metal surface. This means that in those regions, the GO coating was thinner or nonexistent.

Figure 4 - GO coating defect exhibited on the polished surface.

In figure 5, it is possible to see the difference, after 40 layers, between (a) polished surface and (b) textured surfaces with LIPSS. One of the most noticeable things is the lack of graphene in the center of the sample shown in figure 5 (a).

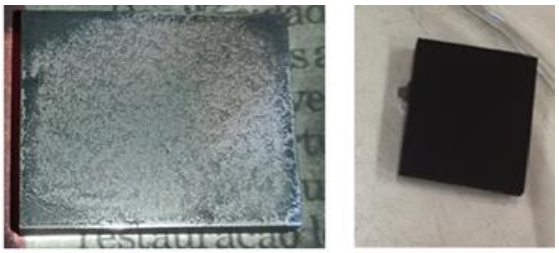

Figure 5 - Surfaces coated with Graphene. (a) polished; (b) LIPSS textured.

A wettability test was done on my LIPSS and allows us to see that the texturized surface becomes hydrophobic and has contact angles higher than 90 degrees. The difference of coating can be explained by the hydrophobic effect combined with the energy/momentum that a atomize drop of Gr solution has after ejection from the nozzle. A stream of compressed air passes through the airbrush; the Venturi effect creates a local reduction in air pressure that allows liquid to be sucked from the dispersion cup. The high velocity of air atomizes the solvent comprised of graphene into very tiny droplets as it blows past the nozzle. On a polished surface, the ejected Gr sheets are transferred from the atomized droplets on to the surface, after we allow the solvent to evaporate and dry. We restart the process, new atomized ejected droplets of Gr dispersion from the nozzle will encounter Gr sheets that are deposited and bonded with weak (Van der Waals) forces to the surface. The droplet energy/momentum is enough to break that bond, and yanks or push/drag the Gr sheet from the initial position. The Gr sheets that overlapped, stacked, or bonded by the liquid medium, coupled with hydrophobic natures of the metal surface, and the deposition angle push/drags Gr in the opposite direction. After the forty layers coat, we attain a lack of Gr in the central section of the sample and a higher graphene concentration at the edges.

On a textured surface, this mechanism/theory acts a little bit differently between LIPSS and the graphene sheet. The atomized Gr droplets enter in contact with the grooves pushing the air trapped between channels out. The droplet energy/momentum is transferred to the Gr sheet and the collision between Gr sheets and the surface generates higher adhesion forces than before. We can even contemplate that some graphene sheets can act as a claw/grip on the grooves or even lodged themselves in the groove's channels. When the second set/layer of atomized Gr droplets is projected from the airbrush and enters in contact with the surface covered with dried Gr sheets bonded with the LIPSS the harder it will be to break the bond between the first graphene sheets and the groove. After an x number of deposition cycles (x number of layers), there will be a uniform/continuous coating. The (x+1) deposition cycle will interact with the graphene coating instead of the grooves.

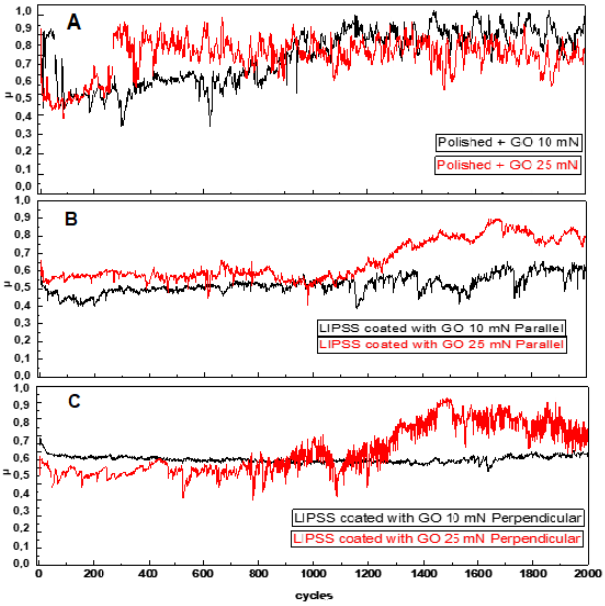

. Figure 6 - Friction coefficient evolution during 2000 cycles with 10 and 25 mN loads for surfaces coated with GO. (A) the polished surface and (B) LIPSS coated with GO and parallel alignment and (C) LIPSS coated with GO and perpendicular alignment.

4.2. Graphene Oxide

Figure 6 shows the friction coefficient evolution for surfaces with GO coatings and 10 and 25 mN loads. (A) the polished surface and (B) LIPSSwith parallel alignment and (C) LIPSS with perpendicular alignment. The LIPSS surfaces have lower COF values and at the 10 mN load, in the parallel direction, between [0.4; 0.5], the lowest COF value observed.

A different behavior can be observed in the polished surfaces that show the lowest coating lifetime. Both alignments have comparable performance. Figure 6 (A) and (C) show an unstable COF attained after the GO coating was damaged. This phenomenon is attributed to the coating destruction and an increase in metal to metal contact.

Figure 7 represents the friction coefficient evolution with 10 and 25 for surfaces coated with GR. (A) the polished surface and (B) LIPSS with parallel alignment and (C) LIPSS with perpendicular alignment. All evolution shows similar behaviors except the LIPSS with10 mN load and perpendicular alignment. The run-in period that consists of a friction coefficient reduction followed by the steady-state regime until the 5000 cycles. However, the COF evolution for 10 mN load with perpendicular alignment shows a continuous growth in friction throughout the test.

The COF attained in 10 mN load and parallel alignment was the lowest observed with COF values between 0.3 and 0.4

.

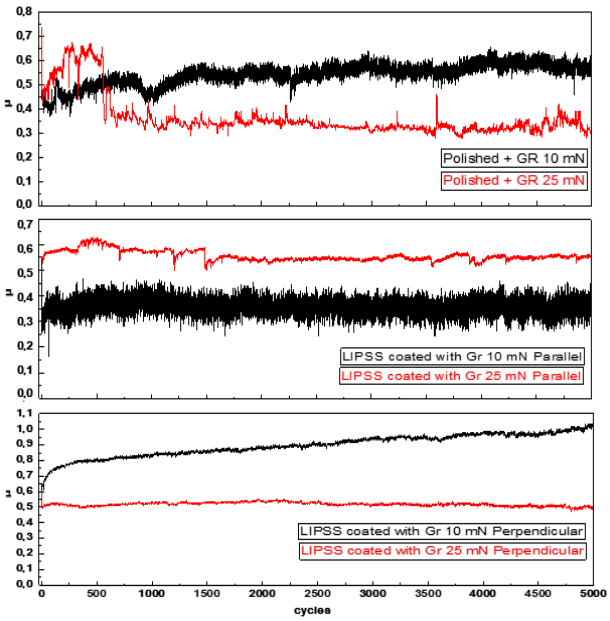

Figure 7 - Friction coefficient evolution during 5000 cycles in a polished surface coated with graphene with 10mN and 25 mN loads.

The wear tracks are similar to each other and have three different zones; the first (I) shows that Gr coating was damaged or pushed to the sides exposing the LIPSS with small Gr areas in the center, (II) the top and bottom part of the wear track appears to have a surface with a smoother look. On the boundaries, we have darker areas that we assume to be created by Gr agglomeration or compressed graphene. Finally, we have a graphene zone surrounding the wear track that corresponds to undamaged or untouched graphene, similar to figure 8.

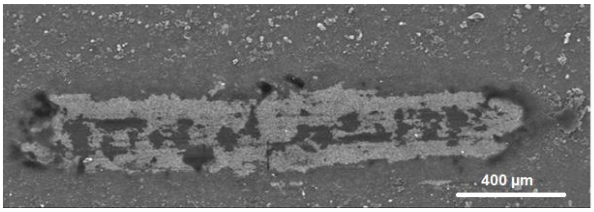

Figure 8 - Wear track obtained after 5000 cycles on LIPSS coated with Gr, done in parallel alignment with 10 mN load and.

5. Conclusions and future work

Comparing all friction coefficient evolutions for polished and textured surfaces with and without GO or Gr coating allows us to state that the introduction of laser-induced periodic structures reduce the COF observed. A considerable reduction in friction coefficient is also seen when both polished and LIPSS surfaces are coated with GO and Gr solid lubricants, showing that LIPSS nanotextured on metallic surfaces can act as reservoirs for graphene-based lubricant.

The lowest friction coefficient attained in polished surfaces was between 0.3 and 0.4 when in the presence of graphene.

In surfaces coated with GO, a similar friction coefficient is observed for both surface treatments and LIPSS directions.

The lowest friction coefficient attained in surfaces coated with Gr was in texturized surfaces with LIPSS with 10 mN load and parallel alignment, similar to the one observed in polished surfaces coated with GR.

5.1. Future work

Future work requires a deeper analysis of mechanisms that are behind friction in LIPSS and graphene-based solid lubricants. These are some ideas that are alluring to try to understand and prove the usage of said systems. After this study, one may conclude that a requirement for the continuation of this work and perform different tests. i.e. to test the higher loads, preparation and analysis of better/different graphene dispersions, a study of other Gr concentrations, development of the same test but using GO powder similar to Gr, improve LIPSS to have better reservoir capability, increase the number of cycles, and study the influence of velocity.

References

[1] V. L. Popov, “Is Tribology Approaching Its Golden Age? Grand Challenges in Engineering Education and Tribological Research,” *Front. Mech. Eng.*, vol. 4, no. November, pp. 1–6, 2018.

[2] J. M. Romano, A. Garcia-Giron, P. Penchev, and S. Dimov, "Triangular laser-induced submicron textures for functionalizing stainless steel surfaces," *Appl. Surf. Sci.*, vol. 440, pp. 162–169, 2018.

[3] F. Fraggelakis, G. Mincuzzi, J. Lopez, I. Manek-Hönninger, and R. Kling, "Controlling 2D laser nanostructuring over a large area with double femtosecond pulses," *Appl. Surf. Sci.*, vol. 470, no. November 2018, pp. 677–686, 2019.

[4] A. Peter, A. H. A. Lutey, S. Faas, L. Romoli, V. Onuseit, and T. Graf, “Direct laser interference patterning of stainless steel by ultrashort pulses for antibacterial surfaces,” *Opt. Laser Technol.*, vol. 123, no. November, p. 105954, 2020.

[5] A. Beatriz, “Comportamento Tribológico de Superfícies Metálicas Nanotexturadas com Lasers de Femtosegundo,” Instituto Superior Técnico, 2017.

[6] J. Bonse, S. V. Kirner, M. Griepentrog, D. Spaltmann, and J. Krüger, “Femtosecond laser texturing of surfaces for tribological applications,” *Materials (Basel).*, vol. 11, no. 5, p. 801, 2018.

[7] K. Holmberg and A. Erdemir, "Global impact of friction on energy consumption, economy, and environment," *FME Trans.*, vol. 43, no. 3, pp. 181–185, 2015.

[8] K. Holmberg and A. Erdemir, “Influence of tribology on global energy consumption, costs and emissions,” *Friction*, vol. 5, no. 3. pp. 263–284, 2017.

[9] A. Cunha, “Multiscale Femtosecond Laser Surface Texturing of Titanium and Titanium Alloys for Dental and Orthopaedic Implants,” Instituto Superior Técnico, 2015.

[10] A. Beltaos *et al.*, "Femtosecond laser-induced periodic surface structures on multi-layer graphene,” *J. Appl. Phys.*, vol. 116, no. 20, pp. 1–6, 2014.

[11] R. Stefan, F. Preusch, and H. Ralf, "Generation of Low-Spatial Frequency Laser-Induced Periodic Surface Structures Driven by Surface Finish," vol. 10, pp. 1–8, 2015.

[12] D. B. Hamilton, J. A. Walowi and C. M. Allen, "A theory of lubrication by micro irregularities," *Wear*, vol. 10, no. 5, p. 412, 1967.

[13] M. Geiger, S. Roth, and W. Becker, "Influence of laser-produced microstructures on the tribological behavior of ceramics," *Surf. Coatings Technol.*, vol. 100–101, no. 1–3, pp. 17–22, 1998.

[14] J. Bonse *et al.*, "Tribological Performance of femtosecond laser-induced periodic surface structures on titanium and a high toughness bearing steel," in *Applied Surface Science*, 2015, vol. 336, pp. 21–27.

[15] J. Bonse, S. V. Kirner, R. Koter, S. Pentzien, D. Spaltmann, and J. Krüger, “Femtosecond laser-induced periodic surface structures on titanium nitride coatings for tribological applications,” *Appl. Surf. Sci.*, vol. 418, pp. 572–579, 2017.

[16] J. Bonse, S. Hohm, S. V Kirner, A. Rosenfeld, and J. Kruger, “Laser-Induced Periodic Surface Structures-A Scientific Evergreen,” *IEEE J. Sel. Top. Quantum Electron.*, vol. 23, no. 3, 2017.

[17] J. Bonse, “Femtosecond laser micromachining of technical materials,” vol. 4065, pp. 161–172, 2004.

[18] Bharat Bhushan, *MODERN HANDBOOK TRIBOLOGY Principles of Tribology*. 2001.

[19] R. J. Yeo, "Ultrathin Carbon-Based Overcoats for Extremely High-Density Magnetic Recording." pp. 1–167, 2017.

[20] M. Berger and M. Seifert, “Nanotechnology. The Future is Tiny.,” *Angewandte Chemie International Edition*, vol. 56, no. 26. pp. 1–359, 2017.